



Original Article

Enhanced relative permittivity in niobium and europium co-doped TiO₂ ceramics

Zhuo Wang*, Haonan Chen, Tian Wang, Yujia Xiao, Wenwen Nian, Jiahao Fan

School of Materials Science and Engineering, Shaanxi University of Science & Technology, Xuefu-Zhonglu 3, Xi'an, 710021, PR China

ARTICLE INFO

Keywords:

Rutile-TiO₂ ceramic
Colossal permittivity
Dielectric relaxation
XPS analysis

ABSTRACT

The appearance of colossal permittivity materials broadened the choice of materials for energy-storage applications. In this work, colossal permittivity in ceramics of TiO₂ co-doped with niobium and europium ions ((Eu_{0.5}Nb_{0.5})_xTi_{1-x}O₂ ceramics) was reported. A large permittivity ($\epsilon_r \sim 2.01 \times 10^5$) and a low dielectric loss ($\tan \delta \sim 0.095$) were observed for (Eu_{0.5}Nb_{0.5})_xTi_{1-x}O₂ ($x = 1\%$) ceramics at 1 kHz. Moreover, two significant relaxations were observed in the temperature dependence of dielectric properties for (Eu, Nb) co-doped TiO₂ ceramics, which originated from defect dipoles and electron hopping, respectively. The low dielectric loss and high relative permittivity were ascribed to the electron-pinned defect-dipoles and electrons hopping. The (Eu_{0.5}Nb_{0.5})_xTi_{1-x}O₂ ceramic with great colossal permittivity is one of the most promising candidates for high-energy density storage applications.

1. Introduction

The continually increasing demands of microelectronics applications have led investigators to be interested in searching for new materials with colossal permittivity [1,2]. In prior decades, much colossal permittivity materials have been investigated, such as BaTiO₃ [3,4], CaCu₃Ti₄O₁₂ [5–9], (Ba, Sr)TiO₃ [10,11], NiO [12], Ba(Fe_{0.5}Nb_{0.5})O₃ [13], K_{0.3}MoO₃ [14] etc. Unfortunately, none of these materials meet the high-energy density storage application requirements.

Recently, a novel colossal permittivity material, (In, Nb) co-doped rutile TiO₂ material was extensively investigated, which possesses high relative permittivity ($> 10^4$) and low dielectric loss (< 0.05) over a very broad temperature range from 80 K to 450 K [15]. In the meantime, the electron-pinned defect dipoles (EPDD) model has been developed to interpret the excellent dielectric performance of (In, Nb) co-doped rutile TiO₂ ceramics. According to the EPDD model, the electron produced by Nb-doping is localized in $2In^{3+} + V_o^{**} + 2Ti^{3+} + 2Nb^{5+} + Ti^{4+}$ defect clusters, which result in the high permittivity and low dielectric loss in (In, Nb) co-doped TiO₂ ceramics [15]. Afterwards, the dielectric properties of other co-doped TiO₂ systems such as Ga³⁺ + Nb⁵⁺ [16], Bi³⁺ + Nb⁵⁺ [17], Sm³⁺ + Ta⁵⁺ [18], Al³⁺ + Nb⁵⁺ [19], Er³⁺ + Nb⁵⁺ [20], Mg²⁺ + Nb⁵⁺ [21], Ca²⁺ + Nb⁵⁺ [22], Zn²⁺ + Nb⁵⁺ [23], Y³⁺ + Nb⁵⁺ [24], Mg²⁺ + Ta⁵⁺ [25] and Sm³⁺ + Nb⁵⁺ [26] co-doped TiO₂ ceramics are investigated, experimental results as shown in Fig. 1. All of these experimental results indicate that co-doped TiO₂ with bivalent or trivalent

ions and pentavalent ions usually present colossal permittivity effect. However, the effect is sensitive to the type of acceptor ions and the concentration of doped ions. Therefore, it is necessary to further research high-performance colossal permittivity material systems using appropriate acceptor and donor co-doped. Hu et al. pointed out that co-doping trivalent In³⁺ ions with a big ionic radius and Nb⁵⁺ ions are favorable to form triangular ($In_2^{3+}V_o^{**}Ti^{3+}$) and diamond shaped ($Nb_2^{5+}Ti^{3+}A_{Ti}(A = Ti^{3+}/In^{3+}/Ti^{4+})$) defect clusters in rutile TiO₂ [15], while an intergrowns, intermediate, and metal-ion-rich structure is founded in co-doping smaller Al³⁺ ions and Nb⁵⁺ ions [27]. Considering the larger ionic radius of Eu³⁺ ions ($r_{Eu} = 108.7$ pm) than In³⁺ ions ($r_{In} = 94$ pm), it is expected to obtain higher permittivity and lower dielectric loss in (Eu, Nb) co-doping TiO₂ by formation larger local defects clusters.

In this work, (Eu_{0.5}Nb_{0.5})_xTi_{1-x}O₂ ($x = 0\%$, $x = 1\%$, $x = 3\%$, $x = 5\%$, $x = 10\%$) ceramics were synthesized by a conventional solid-state reaction. The phase composition and microstructure are carefully characterized. The dielectric permittivity and dielectric loss of the (Eu, Nb) co-doped rutile-TiO₂ as functions of frequency and temperature are systematically studied. High permittivity ($\epsilon_r \sim 2.01 \times 10^5$) and low dielectric loss ($\tan \delta \sim 0.095$) are achieved in (Eu_{0.5}Nb_{0.5})_{0.01}Ti_{0.99}O₂ ceramics. Additionally, XPS results are obtained to evidence the existence of defect dipoles and the correlation between defect dipoles and colossal permittivity.

* Corresponding author.

E-mail address: wangzhou@sust.edu.cn (Z. Wang).

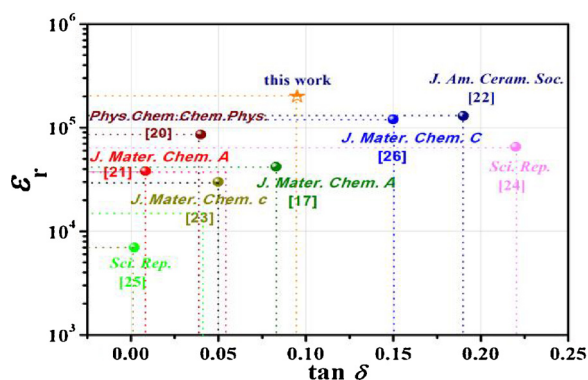


Fig. 1. Comparison of ϵ_r and $\tan\delta$ of co-doped rutile TiO_2 ceramics with different acceptors and donors at 1 kHz.

2. Experimental procedure

Samples of $(\text{Eu}_{0.5}\text{Nb}_{0.5})_x\text{Ti}_{1-x}\text{O}_2$ ($x = 1\%$, 3% , 5% and 10%) were prepared by the solid state sintering method. TiO_2 (98.0%), Nb_2O_5 (99.5%) and Eu_2O_3 (99.99%) were used as raw materials in this work. These raw materials were weighed accurately according to their chemical compositions, and subsequently were mixed by a planetary ball milled for 4 h with deionized water as the medium. All of the mixed powder was calcined at 1200°C for 2 h, and ground in an agate mortar. Then, the mixed powder was pressed into pellets of ~ 10 mm in diameter and ~ 1.0 mm in thickness by cold isostatic pressing process. Finally, these samples were sintered at optimum temperatures to obtain dense ceramics. The sintered samples were pasted silver on both sides and annealed at 650°C for 15 min for electric testing.

Phase composition and crystal structure of these samples were characterized using X-ray diffraction (XRD) (D/max-2200PC Japan) and Raman spectroscopy (Renishaw-invia Britain). Rietveld refinement results of XRD were obtained by the GSAS software. The surface morphology of these samples was observed by field emission-scanning electron microscopy (FE-SEM) (FEI45 + EDAXOctanePrime America). The dielectric properties of these ceramic samples were measured using a precision impedance analyzer (Agilent-E4980A). The oxidation states in $(\text{Eu}_{0.5}\text{Nb}_{0.5})_{0.01}\text{Ti}_{0.99}\text{O}_2$ ceramics were analyzed using X-ray photoelectron spectroscopy (XPS) (AXIS SUPRA Britain). The XPS spectra were fitted by the CasaXPS software.

3. Results and discussion

Fig. 2(a) shows the XRD patterns of $(\text{Eu}_{0.5}\text{Nb}_{0.5})_x\text{Ti}_{1-x}\text{O}_2$ ceramics at different x in the 2θ range of 20° – 80° . The results suggest that a main phase of rutile- TiO_2 is confirmed in all ceramics samples. However, a

small amount of secondary phases is observed in $(\text{Eu}_{0.5}\text{Nb}_{0.5})_x\text{Ti}_{1-x}\text{O}_2$ ceramics with $x > 1\%$, which is owing to that concentration of Eu and Nb ions exceeds over their solubility. According to the Hume-Rothery rule, a substitution solid solution is more likely to be formed if the mismatch of ionic radii is less than 15% [28]. In accordance with this rule, the mismatch of Eu and Ti ionic radii ($|74.5 - 108.7/74.5| = 45.9\%$) is much higher than the in finite solid solution's upper limit, and that of Nb and Ti ionic radii ($|74.5 - 78/74.5| = 5\%$) is far less than the in finite solid solution's upper limit. As a result, Eu^{3+} ions are hard to substitute for the Ti^{4+} ions in the $[\text{TiO}_6]$ octahedron and the secondary phases $\text{Eu}_2\text{Ti}_2\text{O}_7$ and EuNbTiO_6 presented in ceramics. Fig. 2(b) shows Rietveld refinement results of XRD pattern of $(\text{Eu}_{0.5}\text{Nb}_{0.5})_x\text{Ti}_{1-x}\text{O}_2$ ceramics with $x = 1\%$. The ceramics of $x = 1\%$ is determined as a rutile crystal structure of space group P42/mnm with $a = 4.60(1) \text{ \AA}$ and $c = 2.96(5) \text{ \AA}$, where Eu^{3+} ions and Nb^{5+} ions substitute for the Ti^{4+} ions site of TiO_2 .

Fig. 3(a) shows the Raman spectra of $(\text{Eu}_{0.5}\text{Nb}_{0.5})_x\text{Ti}_{1-x}\text{O}_2$ ceramics at different x under excitation with a 532 nm wavelength Ar^+ laser. There are four Raman active fundamental modes: 143 cm^{-1} , 447 cm^{-1} , 612 cm^{-1} and 239 cm^{-1} . 143 cm^{-1} (B_{1g}) corresponds to O–Ti–O bond bending mode, the 447 cm^{-1} (E_g) mode corresponds to oxygen atom liberation along the c -axis out of phase, while 612 cm^{-1} (A_{1g}) corresponds to Ti–O stretch mode [29]. These confirmed the existence of the rutile TiO_2 . Meanwhile, it is noteworthy that the peak at $\sim 239 \text{ cm}^{-1}$ is a multi-phonon peak for the second-order effect [30]. It is generally believed that the peak is induced by the internal stress/strain and partial reduction of the TiO_2 grains. It might be caused by doping elements with different radii in the host lattice. Fig. 3(b) demonstrates the detailed Raman shift of E_g and A_{1g} as functions of doped content x . E_g mode shows a slight blue shift as x increasing, which can directly prove the existence of oxygen vacancies [31]. A_{1g} mode shows a slight red shift as x increasing, which should be attributed to certain factors (e.g., doping, lattice distortion, and partial reduction of the TiO_2 grains [32]). Raman spectroscopy analysis is in consistent with XRD result. The main phase of all ceramic is rutile phase.

Fig. 4 illustrates the dielectric properties of $(\text{Eu}_{0.5}\text{Nb}_{0.5})_x\text{Ti}_{1-x}\text{O}_2$ ceramics at different frequency and compositions. As shown in Fig. 4(a), compared to pure TiO_2 and 0.5% co-doped TiO_2 , other (Eu, Nb) co-doped TiO_2 samples exhibited ultra-high relative permittivity ($> 10^5$), which is superior to the reported materials of (Nb, In) and (Nb, Er) co-doped TiO_2 ($\sim 10^4$) [15,20]. The dielectric properties of TiO_2 samples with co-doped 0.5% (Eu, Nb) similar to that of undoped TiO_2 [33], which may be due to destruction of the intrinsic dipolar effect [34,35]. The mechanism of this phenomenon is not yet clear. Interestingly, $\tan\delta$ of $(\text{Eu}_{0.5}\text{Nb}_{0.5})_x\text{Ti}_{1-x}\text{O}_2$ ceramics with $x > 1\%$ increased with decreasing frequency in a low-frequency range ($< 10^3 \text{ Hz}$) (see Fig. 4(b)). According to the results of XRD patterns, this is possibly attributed to the secondary phase. Fig. 4(c) shows the ϵ_r and $\tan\delta$ of

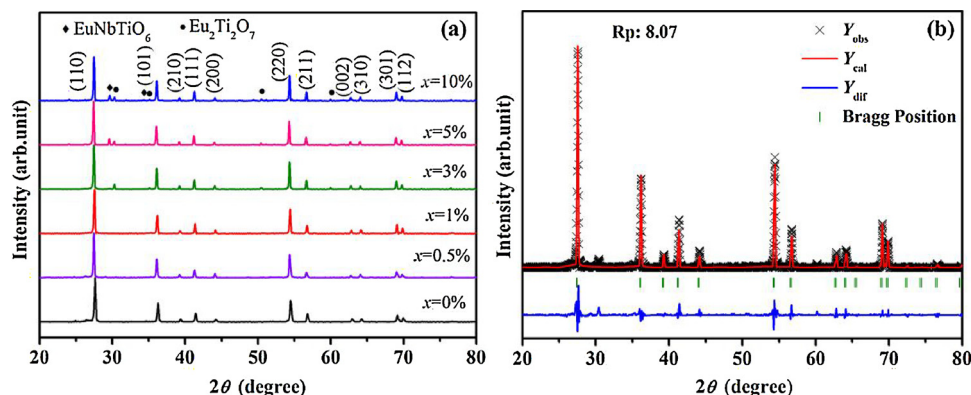


Fig. 2. (a) XRD patterns of $(\text{Eu}_{0.5}\text{Nb}_{0.5})_x\text{Ti}_{1-x}\text{O}_2$ ceramics. (b) Rietveld refinement results of XRD pattern of $(\text{Eu}_{0.5}\text{Nb}_{0.5})_x\text{Ti}_{1-x}\text{O}_2$ ceramics with $x = 1\%$ are given by the GSAS software.

Download English Version:

<https://daneshyari.com/en/article/7897947>

Download Persian Version:

<https://daneshyari.com/article/7897947>

[Daneshyari.com](https://daneshyari.com)